

## ENERGY-SHIFTED LINES IN XMM-NEWTON EPIC SPECTRA OF SEYFERT GALAXIES

A.L.Longinotti<sup>1,2</sup>, S. Sim<sup>1</sup>, K.Nandra<sup>1</sup>, P. O'Neill<sup>1</sup>, and M.Cappi<sup>4</sup>

<sup>1</sup>Astrophysics Group, Imperial College London, Blackett Laboratory Prince Consort Rd, SW7 2AZ London, UK

<sup>2</sup>XMM-Newton Science Operation Centre, ESAC, Apartado 50727 E-28080, Madrid

<sup>4</sup>INAF-IASF Sezione di Bologna, Via Gobetti 101, I-40129 Bologna, Italy

### ABSTRACT

In the recent literature on AGNs it has been often reported that spectra of Seyfert 1 Galaxies show resonant absorption lines of Fe K which are redshifted from the rest frame position. Such lines are often found with marginal significance but, if real, could potentially open up new avenues to study the circumnuclear gas in the black hole environment. It is also extremely important to take them into account in X-ray spectral analysis because of the influence they have in the correct estimation of spectral parameters, Fe K $\alpha$  line *in primis*. An *XMM-Newton* observation of Mrk 335 is reported here as a case study: a narrow feature has been detected at 5.9 keV, i.e. with a redshift corresponding to a velocity of  $v \sim 0.15c$ . Preliminary results on the statistical significance of narrow absorption and emission lines in a sample of PG QSOs observed by *XMM-Newton* are also included.

Key words: AGN, X-rays, spectroscopy.

### 1. INTRODUCTION

Since Active Galactic Nuclei have been discovered, it has been postulated that the powering mechanism is likely to be the release of gravitational energy of matter accreted on a supermassive black hole. Observational evidence for this was found in the redshifted and broad Fe K disc line seen in bright Seyfert galaxies (1). The picture on hard X-ray spectra has been made even more complex by the recent detection of narrow lines shifted from their rest-frame position in the Fe K band spectra of many Seyfert 1 galaxies which may affect modeling of the Fe K emission line. Previous cases of highly ionised redshifted absorption Fe K lines were in fact found superimposed to the broad wing of the Fe K $\alpha$  line in NGC 3516 (2) with *ASCA* data, and in E 1821+643 (3) with *Chandra* data. (4) reported on the presence of an unshifted Fe K absorption line superimposed on the relativistic Fe K line in IRAS13349+2438, with *XMM-Newton* data. High confidence detections of such features would be of crucial im-

portance in testing the black hole paradigm for AGN and would provide a new additional tool to be used alongside the broad Fe K $\alpha$  line. In fact, although the exact nature of the energy shift of such lines is as yet unclear, the most likely scenario for producing the observed features would involve a combination of gas orbiting in highly relativistic motion and/or gravitational shifts of the photons (2; 5). With the advent of *XMM-Newton* and *Chandra*, the number of *absorption* features in active galaxies spectra have considerably increased (6; 3; 7; 8). Narrow energy-shifted *emission* lines have also been detected in the hard X-ray spectra of many AGN (9; 10; 11; 12; 13; 14). Theoretical models have predicted the possibility that Fe K emission lines from the disc can be observed with a narrow profile if the X-ray reflection arises as a result of magnetic flares in localized regions on the disc (15; 16).

### 2. MRK 335 CASE STUDY

#### 2.1. Spectral analysis

Mrk 335 is a bright Seyfert 1 Galaxy at  $z=0.026$ , which was observed by *Xmm-Newton* for about 30 ks. A previous analysis was reported by (17), who found evidence for a broad Fe K $\alpha$  line associated to an ionised reflection component. Here, the data from the pn camera are presented. A fit on the 2-10 keV data with a simple power law model yields a steep spectrum, with  $\Gamma=2.13^{+0.04}_{-0.02}$ . The pn residuals from 3-9 keV are plotted in Fig. 1: the energy band of the Fe K $\alpha$  emission line is pictured on the data showing the presence of broad excess in flux not only above the position of the neutral line (6.4 keV), but even up to  $\sim 7.3$  keV and down to  $\sim 5.9$  keV. A deficit of counts in a notch-shape is also present at  $\sim 5.9$  keV. A Gaussian line is added to the power law, with energy, width and flux free to vary. The line is highly significant with  $\Delta\chi^2=33$  for 3 d.o.f, indicating an ionized and broad line. The line parameters are found to be  $E=6.63^{+0.16}_{-0.14}$  keV (rest-frame),  $\sigma=0.40^{+0.32}_{-0.13}$  keV and  $EW=245^{+123}_{-126}$  eV. Although the residuals shape may suggest the presence of another Gaussian line, any attempt to

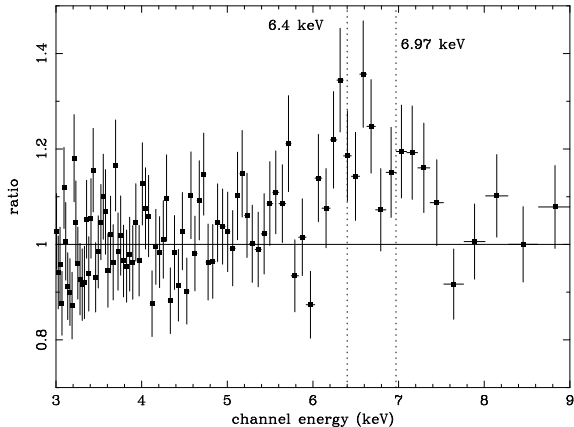


Figure 1. Data to model ratio: the 2-10 keV spectrum is fitted by a power law with  $\Gamma = 2.15^{+0.04}_{-0.03}$ . The plot is in the source rest frame and the Fe  $K\alpha$  energy band is labelled for clarity.

fit the data with 2 emission lines failed. To fit the notch-shaped feature another Gaussian line with negative intensity has been added. The fit yields  $\chi^2 = 738/731$  d.o.f. and the lines parameters are found to be  $E = 6.31^{+0.20}_{-0.20}$  keV,  $\sigma = 0.78^{+0.21}_{-0.26}$  keV,  $EW = 468^{+250}_{-175}$  eV for the broad component and as for the narrow one,  $E = 5.92^{+0.05}_{-0.05}$  keV with an  $EW = 52^{+18}_{-18}$  eV (measured in absorption with negative intensity with respect to the continuum). The width of the absorption line is unresolved with CCD resolution and therefore it is kept fixed to 50 eV. The improvement in  $\chi^2$  is  $\Delta\chi^2 \sim 14$  for 2 degrees of freedom, corresponding to a level of confidence higher than 99.7 percent according to the F-test. This is an extremely basic parametrization of the spectrum, meant purely to show the main features in the spectral curvature above  $\sim 5$  keV. The line profile in fig. 1 appears complex not only for the presence of the absorption feature, but also because the residuals show a double-peak structure. As reported before, fitting *two* emission lines is not required by the fit so we have included only one broad Gaussian in our basic parametrization. When the spectrum is fitted with two Gaussian lines (emission and absorption), the energy of the broad line is consistent with 6.4 keV. A close look to fig. 1, reveals that the profile is very different from a Gaussian and that in this case the use of such model could be quite misleading. The profile is asymmetrical and skewed suggesting that if there is a broad line it could be modified by relativistic effects. We used the DISKLINE model in Schwarzschild metric (18) where the line parameters other than the energy are:  $q$ , the line emissivity index, where the line emissivity  $j$  is a function of the emission radius  $r$  according to  $j \propto r^{-q}$ ; the inner radius  $r_{in}$  and the outer radius  $r_{out}$  of the accretion disc which define the area of the disc where the line is emitted; the inclination of the disc  $i$ , set as to be the angle between the line of sight and the normal to the disc. Fitting the broad line in this way yields  $E = 7.12^{+0.27}_{-0.21}$  keV and  $EW = 407^{+102}_{-109}$  eV,  $q = 3.98^{+2.45}_{-0.77}$ ,  $i = 21^{+8}_{-16}$  and  $\chi^2/\text{d.o.f.} = 735/730$ . The absorption line is included in this fit as a negative Gaussian,

as previously described.

The presence of a diskline suggests that a reflection component should be included. Since the line energy is clearly indicative of a high ionisation state for Iron, the XION model developed by (19) was used to fit the spectrum. In this way, the reflected spectrum is computed in hydrostatic balance, taking into account the ionization instability in the disc. After choosing one of the available geometries, this model calculates the distance between the disc and the source of X-ray photons, the accretion rate, the luminosity of the X-ray source, the inner and outer disc radii and the spectral index as free parameters. Relativistic smearing is included for a non-spinning black hole. We resolved to assume the simplest geometrical configuration (lamppost). After adding an absorption Gaussian line, the model provides a fairly good fit, yielding  $\chi^2/\text{d.o.f.} = 738/730$ .

We try to model the absorption line by adding an appropriate warm absorber to the best fitting reflection model XION. In order to do that, a grid of XSTAR photoionization model was generated with solar elemental abundances and turbulence velocity of 100 km/s. Then, such model has been incorporated in XSPEC as a table model with 3 additional free parameters: i) the column density  $N_w$  ii) the ionization parameter  $\xi$ , which describes the state of the photoionized medium; iii) a redshift parameter which includes all the redshift contributions, namely the cosmological redshift ( $z_{source}$ ), the velocity of the absorber ( $z_{inflow}$ ) and the gravitational shift which the gas may be subjected to, if close enough to the black hole ( $z_{grav}$ ). The best-fitting parameters are consistent with a very ionized absorber, with  $\log \xi \sim 3.9$  ergs  $\text{cm s}^{-1}$  where it is most likely that only the H-like and He-like Fe ions survive. The fit yields  $\chi^2/\text{d.o.f.} = 735/728$ . Four main absorption features are imprinted on the continuum (see Fig. 2): the  $K\alpha$  and  $K\beta$  transitions of Fe XXV and XXVI produce the absorption lines, but only the  $K\alpha$  ones are sufficiently strong to be interesting for our purposes here. The absorption line detected in the data is consistent with the Fe XXVI  $K\alpha$ , whereas the other ones are too weak to be detected at the CCD resolution. Most striking is that, if such feature is identified as we propose, it requires to be redshifted corresponding to an inflow velocity of  $\sim 0.14 c$ . Such value is inferred by measuring the energy shift of the Gaussian line peak ( $\sim 5.92$  keV) from the rest-frame position of 6.90 keV.

## 2.2. A simple model for the inflow

To further investigate the inflow hypothesis, a simple physical model has been developed and used to synthesise X-ray spectra for qualitative comparison with the observed absorption feature (a more thorough description of the model is included in the paper Longinotti et al. in prep.) Spectra were synthesised for the 2 – 10 keV region using a Monte Carlo radiative transfer code based closely on that discussed by (20). For the computation presented here, the power-law photon index was fixed at

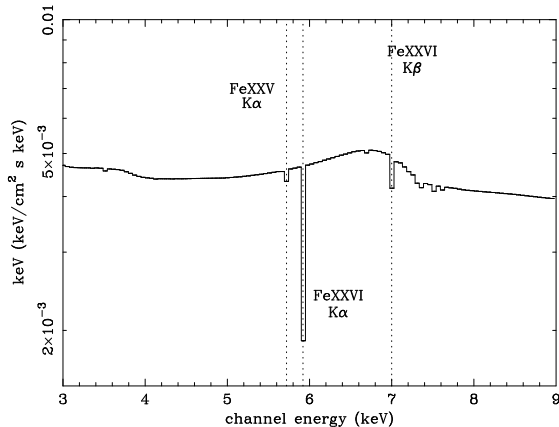


Figure 2. Rest frame plot of the model used to fit the data on the left. The combination of the effects of the reflection spectrum and the highly photoionized gas is visible: the first one reproduces the spectral curvature between 5 and 7 keV, the latter imprints redshifted absorption features on the continuum. In our data, we observe the Fe XXVI  $K\alpha$  only, the other ones being too weak.

$\Gamma = 2.2$  (based on fits to the data) and the normalisation fixed by requiring the total 2 – 10 keV X-ray flux to match the observed luminosity of  $1.8 \times 10^{43}$  ergs  $s^{-1}$ . The disc luminosity was set to 60 per cent of the Eddington luminosity for the central black-hole, close to the value  $L/L_{\text{edd}} = 0.62$  reported for Mrk 335 by (21). The soft-excess was modelled as a black-body with temperature  $1.3 \times 10^6$  K and normalisation fixed to the power-law component. In contrast to that presented by (20), the code used here includes the full special relativistic expression for the Doppler shift and approximately accounts for gravitational redshift using

$$\gamma(1 - \mu v(r)/c)\nu = \nu' \sqrt{1 - 2R_g/r} \quad (1)$$

where  $\nu'$  is the frequency of a photon at radius  $r$  as measured in the comoving frame,  $\mu$  is the usual direction cosine,  $\gamma = (1 - v^2/c^2)^{-1/2}$  and  $\nu$  is the photon frequency that would be recorded by an infinitely distant observer at rest relative to the black-hole. Other relativistic effects are neglected. A simple spherical geometry for the gas in a radial inflow has been considered. It is assumed that the gas occupies a region which extends from inner radius  $r_{\text{in}}$  to outer radius  $r_{\text{out}}$  from the central black-hole. Here only the main results from such model are described. From a qualitative comparison to the computed spectra, the data can rule out an inflow model of a continuous flow extending from the vicinity of the central black-hole to much greater distances. The left panel in Figure 3 shows the 3–9 keV spectrum computed for a model of this sort with  $r_{\text{in}} = 20 R_g$ ,  $r_{\text{out}} = 10^3 R_g$ , and a mass infall rate  $\Phi = 0.2 M_{\odot} \text{ yr}^{-1}$ . This model predicts very few spectral features since the ionisation state of the gas is very high. The dominant feature is a broad inverse P Cygni Fe XXVI  $K\alpha$  line, but a weaker feature due to the  $K\beta$  line of the same ion appears at harder energies. The computed absorption line is very broad, extending from

around 5.5 keV to  $\sim 6.5$  keV, where the deepest absorption occurs. The large line width in the model is therefore the result of the large radial extent of the absorbing gas and of the large velocity range present in the flow. If the infalling gas is instead distributed over a narrow range of radii, the model is found to be a good description of the data (right panel in Figure 3). A possible configuration could be described as a discontinuous infalling of shells or blobs of gas at different densities. With the model considered here, this was obtained by limiting the radial range occupied by the flow.

### 2.3. Significance of the narrow line in Mrk 335

The problem of the reality and significance of narrow features such as the one detected in Mrk 335, has been pointed out in the most recent cases of narrow line detections by (3) for an absorption line, and by (13) for an emission line. These authors have employed realistic Montecarlo simulations for testing the reality of the lines, which have been found significant at a level in between 2-3  $\sigma$ . Moreover, the employment of the F-test to test the significance of X-ray spectral lines has been recently put into question by rigorous statistical arguments (22). Therefore, we try to assess whether the line in Mrk 335 could be due to statistical fluctuations through Montecarlo simulations. The phenomenological model (power law + broad em. line) used in the spectral analysis section, is taken as a “baseline” model and the  $\Delta\chi^2$  for adding an absorption line is measured to be 14.37 in the real spectrum. In this way, 10000 fake background-subtracted data sets have been obtained. Each of these spectra is fitted with the baseline model (power law + broad Gaussian line) and only then, a narrow absorption line with  $\sigma=50$  eV is added to the fit, in order to measure the improvement in  $\chi^2$  with respect to the  $\chi^2$  value obtained by fitting the baseline model with no absorption. We obtain a  $\Delta\chi^2$  larger than in the baseline model in 263 cases, yielding a significance for the absorption line of 97.37 percent.

## 3. SEARCH FOR ENERGY-SHIFTED NARROW LINES: SIMULATION PROCEDURE

All narrow lines detected in the literature have been found in individual sources, as the one discussed for Mrk 335 and many of them have been found marginal. Marginal detections could possibly arise due to random deviations in the spectra. Quantifying the significance of such deviations in a large number of X-ray spectra would provide an estimate of the robustness of the detections. To date, a systematic search for the presence of such features in a sample of objects has not been performed. An attempt to do that is presented in the following. A sample of archival PG quasars observed by *XMM-Newton* has been chosen. For completeness, the description of the X-ray properties of this sample is reported by (23) and (24). In the present analysis instead, only the sources with more than

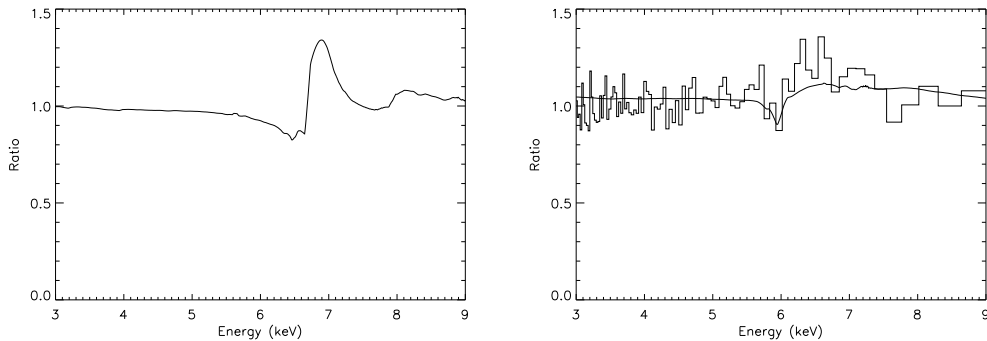


Figure 3. The plot shows the ratio of the computed 3 – 9 keV flux to a power-law with index  $\Gamma = 2.2$  (rest frame energy). Left: inflow with  $r_{in} = 20 R_g$ ,  $r_{out} = 10^3 R_g$ ,  $\Phi = 0.2 M_\odot \text{ yr}^{-1}$ , neglecting radiation pressure. The absorption features are predominantly due to Fe XXVI  $K\alpha$  [around 6.5 keV] and  $K\beta$  [around 7.7 keV]. Right: inflow with  $r_{in} = 24 R_g$ ,  $r_{out} = 48 R_g$ ,  $\Phi = 0.3 M_\odot \text{ yr}^{-1}$ , accounting for radiation pressure due to electrons at 60 per cent of the Eddington limit. The absorption feature is due to FE XXVI  $K\alpha$ . The light histogram shows the observational data for Mrk 335, also normalised to a power-law fit

800 counts above 5 keV are included in order to insure good statistics in the Fe K region. The list of the sources is shown in Table 1. A blind search for positive and negative flux deviations has been performed in the simulated spectra. This procedure is addressed to test for the presence of a narrow line in each of the spectra in the sample. We shall distinguish between unshifted Fe K lines (i.e. emission lines in the range 6.4-7 keV) and those which we will call energy-shifted lines, i.e. any absorption line and emission lines shifted out of this range.

- For each spectrum, 10000 spectra have been simulated with XSPEC assuming a baseline model *without* any narrow line, folding it through the same instrumental response and adding Poisson noise. Such spectra have then been grouped according to the same criterion adopted for the real data set, i.e. 20 counts per spectral bin. In this way, 10000 synthetic background-subtracted spectra were generated, with photon statistics corresponding to the exposure in the pn detector (see second column in Table 1).
- Each of these spectra was fitted first with the baseline model. Then, each of them was fitted a second time with a model consisting of the baseline model plus a narrow line. The narrow line parameters were set as follows. Positive and negative deviations were allowed for the line flux. The width of the narrow line was fixed to 50 eV during the fitting and the energy of the line was stepped in steps of 70 eV, corresponding approximately to the instrumental resolution. To avoid any calibration uncertainties at the boundaries of the instrumental response, the line is searched across the energy range 2.5–9.5 keV. For each energy on this grid, the value of the  $\Delta\chi^2$  for adding the narrow line to the data was calculated with respect to the baseline model. When the minimum  $\Delta\chi^2$  was found, the values of the corresponding energy and line flux were recorded. In this way, the most significant narrow lines in the data were

detected.

- The presence of a narrow feature has been tested in the *real* spectrum applying the same grid of energy, so that the comparison is made consistently.
- The procedure of fitting the spectrum with the baseline model and then adding a narrow line with the same grid of energies described above, has been repeated for each simulated spectrum. In each of the fake data sets, the greatest improvement in  $\chi^2$  for adding the narrow feature,  $\Delta\chi^2(\text{sim})$ , is recorded, along with the energy and the flux of the line, providing a list of 10000 detections. Then, the number of spectra where  $\Delta\chi^2(\text{sim}) > \Delta\chi^2(\text{data})$  is counted. This quantifies the probability that an apparent feature as significant as that in the real data could be the result of random noise.

Two runs of simulations have been performed. The first run picks up the most significant line in each spectrum, with the adopted baseline model. The second run is performed for a limited number of spectra where an unshifted emission Fe  $K\alpha$  line has been detected at >90% in the first run. In these cases, the Fe K line has been added to the baseline model and the procedure has been run again. Table 2 summarises the final results and the baseline model used for each spectrum.

This table comprises the list of the 10 detections significant at >90% selected in the following way:

- Energy-shifted features significant at >90% from the first run of simulations
- Energy-shifted features significant at >90% from the second run of simulations (i.e. after including significant Fe  $K\alpha$  lines in the baseline model)

Table 1. List of the PG QSOs sample where the narrow lines blind search has been performed. The sources have been fitted with a power law in the 2-10 keV range.

Quasar	Exposure	Gamma	Flux	$\chi^2$ /d.o.f.
-	s	-	( $10^{-12}$ cgs)	-
Mrk 335	28401	$2.12^{+0.02}_{-0.02}$	11.81	815/742
IIIZW2	10141	$1.62^{+0.04}_{-0.04}$	6.78	344/349
I Zw 1	18189	$2.29^{+0.03}_{-0.03}$	7.73	529/450
PG 0844+349	9230	$2.07^{+0.07}_{-0.07}$	4.69	169/172
PG 0947+396	17392	$1.90^{+0.06}_{-0.05}$	1.75	197/217
PG 0953+414	10211	$2.07^{+0.05}_{-0.05}$	2.92	194/225
PG 1048+342	19801	$1.82^{+0.06}_{-0.07}$	1.32	196/197
PG 1114+445	34902	$1.46^{+0.03}_{-0.04}$	2.23	363/386
PG 1115+080	37082	$1.89^{+0.06}_{-0.06}$	0.26	178/184
PG 1202+281	11448	$1.72^{+0.05}_{-0.05}$	3.60	216/241
PG 1211+143	46884	$1.73^{+0.02}_{-0.02}$	3.06	741/638
PG 1407+265	46124	$2.45^{+0.02}_{-0.02}$	1.34	465/490
PG 1415+451	20569	$1.99^{+0.07}_{-0.08}$	1.09	151/159
PG 1425+267	29394	$1.48^{+0.04}_{-0.04}$	1.65	337/312
PG 1427+480	30763	$1.98^{+0.06}_{-0.06}$	1.04	246/251
Mrk 478	18037	$2.12^{+0.06}_{-0.06}$	1.84	189/202
PG 1448+273	17840	$2.23^{+0.06}_{-0.06}$	2.09	239/245
Mrk 841(*)	7609	$1.92^{+0.03}_{-0.03}$	14.80	468/492
PG 1512+370	13503	$1.81^{+0.06}_{-0.06}$	1.86	226/216
PG 1634+716	12207	$2.25^{+0.06}_{-0.06}$	0.74	267/207
UGC 11763	23579	$1.63^{+0.04}_{-0.04}$	3.68	361/423
Mrk 304	6945	$0.88^{+0.06}_{-0.08}$	3.41	224/115

(\*)3 spectra in the archive

In total, 10 detections out of 24 spectra have been found at a significance higher than 90%.

To estimate the probability to detect 10 features by random chance, it is assumed a null hypothesis in which the sample comprises 24 featureless spectra. The probability that this hypothesis can be rejected in the present data is then calculated assuming the binomial distribution as a probability distribution:

$$P = \frac{n!}{x!(n-x)!} p^x (1-p)^{n-x} \quad (2)$$

In the present case, the parameters of the distribution correspond to  $n=24$  (number of spectra),  $x=10$  (number of successes i.e. detections at  $>90\%$ ),  $p=0.1$  (i.e. the probability to have a detection at more than 90% in the case of the null hypothesis). The cumulative probability for a given number of random detections defines the probability to have  $up$  to that number of random detections in the sample and it is defined as:

$$P_c = \sum_{k=0}^x p_f$$

The probability to find 10 or more random detections in the sample is calculated to be  $1-P_c=5.25 \times 10^{-5}$ . This number is very small, implying that it is very unlikely that 10 detections in a sample of 24 spectra are all due to random noise. Therefore, the possibility that none of them is real can be ruled out, i.e. the null hypothesis

Table 2. List of the shifted features detected at  $> 90\%$  in each spectrum with the corresponding baseline model

Quasar	Baseline	Energy (*)	Intensity (*)	Significance
-	-	(keV)	( $\text{Ph s}^{-1} \text{cm}^{-2}$ )	-
Mrk 335	plaw+broad gau	5.93	-7.422e-06	95.82%
IIIZW2	plaw	9.01	-5.870e-06	90.93%
I Zw 1	plaw	3.20	-1.187e-05	96.34%
PG 1211+143	plaw+zwabs	7.61	-2.9541e-06	100%
PG 1211+143	plaw+zwabs+2 zgau	2.92	-7.411e-06	99.96%
PG 1407+265	plaw	7.89	3.794e-06	92.2%
Mrk 841 (I)	plaw	6.28	1.504e-05	98.26%
PG 1634+716	plaw	4.11	-1.109e-5	96.99%
UGC 11763	plaw	6.28	3.781e-06	94.21%
Mrk 304	plaw+zwabs +zgau	4.46	9.986e-06	100%

is rejected. From statistical considerations, it is reasonable saying that out of 10 detections *some* are real. From a more speculative point of view, let us considering the number of successful events characterised by the average cumulative probability  $P_c=0.5$ . At this point, it is as likely to have *more* than  $x$  false detections, as to have *less* than  $x$  false detections, because obviously they have the same cumulative probability. For 24 number of trials, the probability calculation shows that such number is between 2 and 1. So, one could draw an approximate conclusion by saying that the majority of the 10 detections are real, at a level of confidence of 90% and 2-3 of them are false.

#### 4. SUMMARY OF RESULTS

A narrow absorption line has been detected at  $\sim 5.9$  keV with a significance of  $\sim 97\%$  in the EPIC pn spectrum of Mrk 335; if interpreted as Fe XXVI  $K\alpha$  and if the effect of the gravitational field is neglected, the observed redshift of the line corresponds to a receding velocity of  $50000 \text{ km s}^{-1}$  in the absorbing gas. The comparison to a physical inflow model shows that the line is consistent with being produced in a discontinuous flow of material dragged in high velocity motion towards the nucleus, rather than in a spherical flow. Arguably, the fact that the line is not smeared nor broad is a strong indication against the hypothesis of matter in orbit at a few gravitational radii, as suggested for other similar cases.

The blind search for energy shifted features carried out in the sample of PG quasars provided an encouraging result on the statistical significance of the narrow lines, in general. The majority of the detections are in fact believed to be real in the *XMM-Newton* data. This preliminary result should be investigated using a much larger sample of spectra.

## ACKNOWLEDGMENTS

The AstroGroup at Imperial College London is acknowledged for financial support. A.L.L. is grateful to Giovanni Miniutti for many stimulating discussions during this conference.

## REFERENCES

- [1] Nandra, K., George, I. M., Mushotzky, R. F., Turner, T. J., and Yaqoob, T. ASCA Observations of Seyfert 1 Galaxies. II. Relativistic Iron K alpha Emission. *ApJ*, 477:602–+, March 1997.
- [2] Nandra, K., George, I. M., Mushotzky, R. F., Turner, T. J., and Yaqoob, T. The Properties of the Relativistic Iron K-Line in NGC 3516. *ApJ*, 523:L17–L20, September 1999.
- [3] Yaqoob, T. and Serlemitsos, P. Iron K Features in the Quasar E1821+643: Evidence for Gravitationally Redshifted Absorption? *ApJ*, 623:112–122, April 2005.
- [4] Longinotti, A. L., Cappi, M., Nandra, K., Dadina, M., and Pellegrini, S. The complex FeK line of the Narrow-Line Seyfert 1 galaxy IRAS 13349+2438. *A&A*, 410:471–479, November 2003.
- [5] Ruszkowski, M. and Fabian, A. C. On the influence of resonant absorption on the iron emission-line profiles from accreting black holes. *MNRAS*, 315:223–228, June 2000.
- [6] Matt, G., Porquet, D., Bianchi, S., Falocco, S., Maiolino, R., Reeves, J. N., and Zappacosta, L. A changing inner radius in the accretion disc of Q0056-363? *A&A*, 435:857–861, June 2005.
- [7] Dadina, M., Cappi, M., Malaguti, G., Ponti, G., and De Rosa, A. X-ray absorption lines suggest matter infalling onto the central black-hole of mrk 509. *astro-ph/0506697*, 2005.
- [8] Reeves, J. N. et al. Evidence for gravitational infall of matter onto the super- massive black hole in the quasar pg 1211+143? 2005.
- [9] Turner, T. J., Mushotzky, R. F., Yaqoob, T., George, I. M., Snowden, S. L., Netzer, H., Kraemer, S. B., Nandra, K., and Chelouche, D. Narrow Components within the Fe K $\alpha$  Profile of NGC 3516: Evidence of the Importance of General Relativistic Effects? *ApJ*, 574:L123–L127, August 2002.
- [10] Turner, T. J., Kraemer, S. B., and Reeves, J. N. Transient Relativistically Shifted Lines as a Probe of Black Hole Systems. *ApJ*, 603:62–66, March 2004.
- [11] Guinazzi, M. The history of the iron K line profile in the Piccinotti AGN ESO 198-G24. *A&A*, 401:903–910, April 2003.
- [12] Yaqoob, T., George, I. M., Kallman, T. R., Padmanabhan, U., Weaver, K. A., and Turner, T. J. Fe XXV and Fe XXVI Diagnostics of the Black Hole and Accretion Disk in Active Galaxies: Chandra Time-resolved Grating Spectroscopy of NGC 7314. *ApJ*, 596:85–104, October 2003.
- [13] Porquet, D., Reeves, J. N., Uttley, P., and Turner, T. J. XMM-Newton observation of the Seyfert 1.8 ESO 113-G010: Discovery of a highly redshifted iron line at 5.4 keV. *A&A*, 427:101–105, November 2004.
- [14] Gallo, L. C., Fabian, A. C., Boller, T., and Pietsch, W. A possible line-like emission feature at 8 keV in the Seyfert 1.2 UGC 3973. *MNRAS*, pages 732–+, August 2005.
- [15] Nayakshin, S. and Kazanas, D. Narrow Moving Fe K $\alpha$  Lines from Magnetic Flares in Active Galactic Nuclei. *ApJ*, 553:L141–L144, June 2001.
- [16] Dovčiak, M., Bianchi, S., Guinazzi, M., Karas, V., and Matt, G. Relativistic spectral features from X-ray-illuminated spots and the measure of the black hole mass in active galactic nuclei. *MNRAS*, 350:745–755, May 2004.
- [17] Gondoin, P., Orr, A., Lumb, D., and Santos-Lleo, M. XMM-Newton observations of the Seyfert 1 galaxy Mrk 335. *A&A*, 388:74–87, June 2002.
- [18] Fabian, A. C., Rees, M. J., Stella, L., and White, N. E. X-ray fluorescence from the inner disc in Cygnus X-1. *MNRAS*, 238:729–736, May 1989.
- [19] Nayakshin, S. and Kallman, T. R. Accretion Disk Models and Their X-Ray Reflection Signatures. I. Local Spectra. *ApJ*, 546:406–418, January 2001.
- [20] Sim, S. A. Modelling the X-ray spectra of high-velocity outflows from quasars. *MNRAS*, 356:531–544, January 2005.
- [21] Gierliński, M. and Done, C. Is the soft excess in active galactic nuclei real? *MNRAS*, 349:L7–L11, March 2004.
- [22] Protassov, R., van Dyk, D. A., Connors, A., Kashyap, V. L., and Siemiginowska, A. Statistics, Handle with Care: Detecting Multiple Model Components with the Likelihood Ratio Test. *ApJ*, 571:545–559, May 2002.
- [23] Piconcelli, E., Jimenez-Bailón, E., Guinazzi, M., Schartel, N., Rodríguez-Pascual, P. M., and Santos-Lleo, M. The XMM-Newton view of PG quasars. I. X-ray continuum and absorption. *A&A*, 432:15–30, March 2005.
- [24] Jiménez-Bailón, E., Piconcelli, E., Guinazzi, M., Schartel, N., Rodríguez-Pascual, P. M., and Santos-Lleo, M. The XMM-Newton view of PG quasars. II. Properties of the Fe K $\alpha$  line. *A&A*, 435:449–457, May 2005.